

Learning Argo profiles by using the signature method

Nozomi Sugiura¹ and Shigeki Hosoda¹

¹Research and Development Center for Global Change, JAMSTEC, Yokosuka, Japan

Correspondence to: Nozomi Sugiura (nsugiura@jamstec.go.jp)

Abstract. A profile from the Argo ocean observation array is a sequence of three-dimensional vectors composed of pressure, salinity, and temperature, appearing as a continuous curve in three-dimensional space. The shape of this curve is faithfully represented by a path signature, which is a collection of all the iterated integrals. Moreover, the product of two terms of the signature of a path can be expressed as the sum of higher-order terms. Thanks to this algebraic property, a nonlinear function of profile shape can always be represented by a weighted linear combination of the iterated integrals, which enables machine learning of a complicated function of the profile shape. In this study, we performed supervised learning for existing Argo data with quality control flags by using the signature method, and demonstrated the prediction skill by cross-validation. Unlike rule-based approaches, which requires several complicated and possibly subjective rules, this method is simple and objective in its nature because it relies only on past knowledge regarding the shape of profiles. This technique should be critical to realizing automatic quality control for Argo profile data.

1 Introduction

Argo is an international effort collecting high-quality temperature and salinity profiles from typically the upper 2000 m of the global ocean (Gould et al., 2004). The data come from battery-powered autonomous floats that drift mostly at a depth, where they are stabilized at a constant pressure level. At typically 10-day intervals, the floats rise to the surface for approximately 6 h while measuring temperature and salinity. On surfacing, the satellites position the floats and receive the transmitted data. Now, the array of over 3000 floats provides 100,000 temperature/salinity profiles per year distributed over the global oceans at an average 3-degree spacing. The quality control of the massive Argo profile data (ARGO, 2019) must be systematic to keep the quality of the observational data homogeneous, and to utilize human resources efficiently. In addition, accurately quantifying the relationship between the profile shape and the effect it has on oceanic processes is essential for understanding the ocean state through the profile observation. Conventionally, much time and effort is spent assigning the quality control flag to each Argo profile. To raise the efficiency of this task, attempts have been made to automate the quality control in a rule-based manner (e.g., Ono et al., 2015; Hayashi et al., 2016; Kamikawaji et al., 2016). As an alternative and more flexible approach, this study attempted to automate the process by supervised learning of the human judgment process. In doing so, it is essential to quantify the profile shape so that the function that yields the quality control flag can be expressed as a linear combination of the numerical values that represent the profile shape. The machine learning thereby reduces to a linear optimization problem

that can be easily solved. The key tool that enables this quantification is the signature, which is the set of all iterated integrals (Chevyrev and Kormilitzin, 2016; Levin et al., 2013), proposed in the theory of rough path by Lyons et al. (2007).

In this research, we propose a procedure of first converting the vector sequence of each Argo profile into a sequence of real numbers that represents its shape, and then expressing a nonlinear function of the shape in the form of a linear combination of these numbers; this conversion facilitates machine learning of the nonlinear function. A machine learning experiment regarding the function was performed and applied to automatic assignment of quality control flags to the profiles.

2 Theoretical background

To understand the notion of signature, consider how the theory of rough path treats a data sequence acting on a system. In this paper, the subscript notation Y_τ is used to denote dependence on the parameter $\tau \in [0, t]$; $A^{\bullet n}$ and $A^{\otimes n}$ denote the n -th power and n -times tensor product, respectively, but otherwise a superscript denotes a component. Suppose we have a system of ordinary differential equations with respect to Y_τ forced by a path X_τ :

$$dY_\tau^i = \sum_{j,k} F_{jk}^i Y_\tau^j dX_\tau^k, \quad (1)$$

where Y_τ^j is the j -th component of vector Y_τ , and F_{jk}^i is the i, j, k -th component of 3-dimensional tensor F .

Performing the Picard iteration yields a solution:

$$Y_t^i = \sum_{n=0}^{\infty} \sum_{i, j, k} F_{i_{n-1}k_n}^i \cdots F_{i_1k_2}^{i_2} F_{jk_1}^{i_1} X_n^{(k_1k_2\cdots k_n)} Y_0^j, \quad (2)$$

where $X_n^{(k_1k_2\cdots k_n)} \stackrel{\text{def}}{=} \int_{0 < \tau_1 < \cdots < \tau_n < t} dX_{\tau_1}^{k_1} dX_{\tau_2}^{k_2} \cdots dX_{\tau_n}^{k_n}$ is a component of the n -th iterated integral

$$\mathbf{X}_n \stackrel{\text{def}}{=} \int_{0 < \tau_1 < \cdots < \tau_n < t} dX_{\tau_1} \otimes dX_{\tau_2} \otimes \cdots \otimes dX_{\tau_n}. \quad (3)$$

By omitting the indices, we can simply write the solution as $Y_t = [\sum_{n=0}^{\infty} F^{\otimes n} \mathbf{X}_n] Y_0$. Notice that the convergence of the series is guaranteed because the magnitude of each iterated integral is uniformly bounded: $|X_n^{(k_1k_2\cdots k_n)}| < \frac{L^{\bullet n}}{n!}$, where L is the path length. This form of solution suggests that the action of X on Y can be well summarized by the iterated integrals, and an approximate solution is reproduced by a truncated series of iterated integrals $(\mathbf{X}_0, \mathbf{X}_1, \cdots, \mathbf{X}_n)$, which is called a truncated signature up to order n . The situation is similar even if $F(Y, dX)$ is a nonlinear function, owing to the shuffle-product property, which is explained later. The point is that the effect of a forcing on a system is asymptotically approximated by the truncated path signature, but not by the partial sequence of state vectors.

3 Method

The data used in this research were observed by the global array of Argo floats (ARGO, 2019), each of which floats and sinks from the sea surface to approximately 2000m depth. Figure 1 shows examples of the vertical profiles of temperature, salinity,

and pressure. By virtue of quality control procedures with manual judgment, the quality control flags are already assigned to all of the data.

Here, we describe the basic concept of the signature method, and how to apply it to Argo profiles. We also explain how to construct a procedure for supervised learning using the signature and how to verify the results.

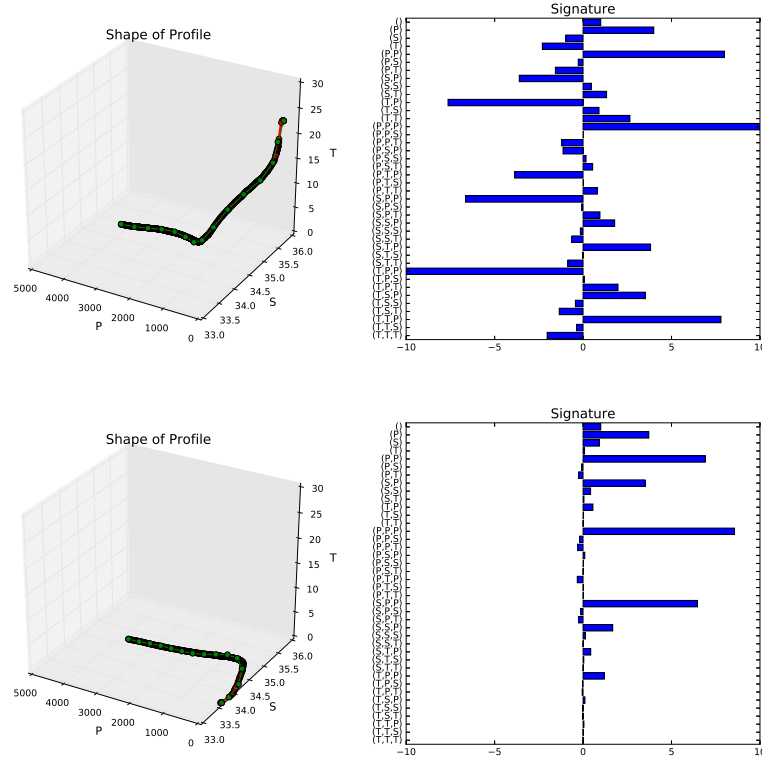


Figure 1. Examples of profile shape obtained from Argo observation (left), and their first few iterated integrals (right).

3.1 Representing the Argo profile shape by signature

3.1.1 Definition of signature

Characteristics of a data sequence can be represented by the signature, which comprises the iterated integrals. Suppose we have a sequence of d -dimensional vectors X_u ($0 \leq u \leq t$). Let the time order be $0 < t_1 < \dots < t_n < t$. We define the iterated integral for indices $i_1, \dots, i_n = 1, \dots, d$ as

$$X^{(i_1 \dots i_n)} = \int_{t_n=0}^t \dots \int_{t_1=0}^{t_2} dX_{t_1}^{i_1} \dots dX_{t_n}^{i_n}. \quad (4)$$

By treating all the index values together, we obtain a tensor of order n :

$$\mathbf{X}^n = \int_{0 < t_1 < \dots < t_n < t} dX_{t_1} \otimes \dots \otimes dX_{t_n} \quad n = 1, 2, \dots, \quad (5)$$

and \mathbf{X}^0 is constant 1. It is important that this encodes the order in which each component changes along the path.

Moreover, by putting together the iterated integrals for all combinations of the indices, we obtain the signature up to degree n :

$$\mathcal{S}^n(X) = (\mathbf{X}^0, \mathbf{X}^1, \mathbf{X}^2, \dots, \mathbf{X}^n), \quad (6)$$

which has $(d^{n+1} - 1)/(d - 1)$ components.

For two signatures, $\mathcal{S}^n(X) = (\mathbf{X}^0, \mathbf{X}^1, \dots, \mathbf{X}^n)$ and $\mathcal{S}^n(Y) = (\mathbf{Y}^0, \mathbf{Y}^1, \dots, \mathbf{Y}^n)$, we can define the product as

$$\mathcal{S}^n(X) \otimes \mathcal{S}^n(Y) \stackrel{\text{def}}{=} (\mathbf{Z}^0, \mathbf{Z}^1, \dots, \mathbf{Z}^n), \quad (7)$$

$$\mathbf{Z}^n = \sum_{k=0}^n \mathbf{X}^k \otimes \mathbf{Y}^{n-k}, \quad (8)$$

whose components are

$$Z^{(i_1 \dots i_n)} = \sum_{k=0}^n X^{(i_1 \dots i_k)} Y^{(i_{k+1} \dots i_n)}. \quad (9)$$

The set of signatures has a group structure in the free tensor algebra with respect to the product \otimes .

3.1.2 Computation of signature

By treating profile data X_u ($0 \leq u \leq t$) as a line graph, we can compute its iterated integrals as follows:

1. For line segment $X_u^i = X_0^i + X_{0,t}^i u$, $0 \leq u \leq t$, which has starting point X_0^i and slope $X_{0,t}^i$, the iterated integral is calculated as

$$\begin{aligned} X^{(i)} &= t X_{0,t}^i, & X^{(ij)} &= \frac{t^{\bullet 2}}{2!} X_{0,t}^i X_{0,t}^j, \\ X^{(ijk)} &= \frac{t^{\bullet 3}}{3!} X_{0,t}^i X_{0,t}^j X_{0,t}^k, \end{aligned} \quad (10)$$

and the 0-th iterated integral is constant 1. In this case, the signature is nothing but a commutative exponential function for the vector $X_{0,t}$:

$$\mathcal{S}(X_{0,t}) = \sum_{n=0}^{\infty} \frac{t^{\bullet n}}{n!} \sum_{i_1, i_2, \dots, i_n} \prod_{k=1}^n X_{0,t}^{i_k} \mathbf{e}_{i_k}. \quad (11)$$

2. Let the time order be $s \leq u \leq t$. By concatenating a path $X_{s,u}$ from time s to u with a path $X_{u,t}$ from time u to t , we obtain a path $X_{s,t}$ from time s to t , whose signature is the product of the signatures:

$$\mathcal{S}(X_{s,t}) = \mathcal{S}(X_{s,u}) \otimes \mathcal{S}(X_{u,t}). \quad (12)$$

This equation defines a homomorphism from path space with concatenation to signature space with the group operation; this is called Chen's identity (Chen, 1958).

3. By concatenating the paths successively using Eq. (12), we can compute the signature for the whole line graph.

The numerical computation of the signature in this study is performed by using Python library `Esig` (Kormilitzin, 2017).

3.1.3 Lead-lag transformation

Suppose we have a sequence of d -dimensional ($d = 3$) vectors with length $N + 1$:

$$X = (X_0, X_1, \dots, X_N) = \left(\begin{bmatrix} P_0 \\ S_0 \\ T_0 \end{bmatrix}, \begin{bmatrix} P_1 \\ S_1 \\ T_1 \end{bmatrix}, \dots, \begin{bmatrix} P_N \\ S_N \\ T_N \end{bmatrix} \right)$$

To more precisely grasp the shape of the line graph, we perform a lead-lag transformation (Chevyrev and Kormilitzin, 2016), which defines a sequence of $2d$ -dimensional vectors with length $N \cdot 2d + 1$:

$$\begin{bmatrix} P_0 \\ S_0 \\ T_0 \\ P_0 \\ S_0 \\ T_0 \end{bmatrix}, \begin{bmatrix} P_1 \\ S_0 \\ T_0 \\ P_0 \\ S_0 \\ T_0 \end{bmatrix}, \begin{bmatrix} P_1 \\ S_1 \\ T_0 \\ P_0 \\ S_0 \\ T_0 \end{bmatrix}, \begin{bmatrix} P_1 \\ S_1 \\ T_1 \\ P_0 \\ S_0 \\ T_0 \end{bmatrix}, \dots, \begin{bmatrix} P_1 \\ S_1 \\ T_1 \\ P_1 \\ S_1 \\ T_1 \end{bmatrix}, \begin{bmatrix} P_2 \\ S_1 \\ T_1 \\ P_1 \\ S_1 \\ T_1 \end{bmatrix}, \begin{bmatrix} P_2 \\ S_2 \\ T_1 \\ P_1 \\ S_1 \\ T_1 \end{bmatrix}, \dots, \begin{bmatrix} P_N \\ S_N \\ T_N \\ P_N \\ S_N \\ T_{N-1} \end{bmatrix}, \begin{bmatrix} P_N \\ S_N \\ T_N \\ P_N \\ S_N \\ T_N \end{bmatrix}.$$

The transition rule for the lead-lag transformation is as follows:

1. Take **two copies** of X_0 , and use it as the initial condition.
2. Update **only 1 component** among $2d$ components at once.
3. Use the previous value instead if the present value is missing.

3.2 Machine learning procedure for quality control process

Suppose we have a set of profile data $X(m) \stackrel{\text{def}}{=} \{X_u(m) | 0 \leq u \leq 1\}$ for $m = 1, 2, \dots, M$, whose signature is denoted as $X(m) \stackrel{\text{def}}{=} \mathcal{S}(X(m))$. Let us consider the problem of assigning the discriminant values to each profile depending on whether a profile matches the quality standard.

1. We first make a model for the rule of quality control as a functional form; that is, a linear combination of the iterated integrals X^I for all combinations of indices $I = (i_1), (i_1 i_2), \dots, (i_1 \dots i_n)$ yields the discriminant value.

$$y = \sum_I w^I X^I + \epsilon^I, \tag{13}$$

where ϵ is the error. Such a representation is possible because its nonlinearity is unraveled thanks to the property of shuffle product; for a fixed path X , the product of iterated integrals for indices A and B is expressed by the iterated integral with respect to the shuffle product $A \sqcup B$:

$$X^A X^B = X^{A \sqcup B}. \quad (14)$$

For example, $X^{(aa)} X^{(b)} = X^{(baa)} + X^{(aba)} + X^{(aab)}$. This means that a product of iterated integrals is always reduced to the sum of higher-order iterated integrals. Moreover, by virtue of the Stone–Weierstrass theorem, any nonlinear function of the shape of a path can be represented as a linear combination of the iterated integrals.

2. Suppose we have pairs $(X(m), y(m))$, where each $X(m)$ is a profile sequence, and $y(m) = 0, 1$ is the discrimination value, which is already given to each sample $m = 1, 2, \dots, M$ as learning data. Learning these data is nothing but deriving the weights w^I that minimize an L_1 -regularized cost function:

$$J(w) = \frac{1}{2M} \sum_{m=1}^M \left(y(m) - \sum_I w^I X(m)^I \right)^2 + \alpha \sum_I |w^I|. \quad (15)$$

3. Using the coefficients w derived in (15), and substituting into Eq(13) the iterated integrals for a profile not used for learning, we obtain \hat{y} , an estimation for y (cross-validation).
4. The minimization problem is efficiently solved by the coordinate descent (CD) method (Friedman et al., 2007).

For the L_1 -regularization term to apply evenly, each iterated integral X^I is preprocessed by subtracting the ensemble mean μ_{train} of the training ensemble and dividing by the standard deviation σ_{train} of the training ensemble:

$$X(m)^I \leftarrow \frac{X(m)^I - \mu_{\text{train}}}{\sigma_{\text{train}}}. \quad (16)$$

The same operation is performed for the iterated integrals in cross-validation. The minimization problem is solved by using the Python library `scikit-learn` (Pedregosa et al., 2011).

3.3 Assessment of learning results

The performance of the binary classifier can be quantitatively assessed by visualizing it with the receiver operating characteristic (ROC) curve (Egan, 1975). We call the profiles that pass the quality criterion negative $y = 1$, and otherwise positive $y = 0$. By shifting the cutoff value y_c , one can count the number of positive ones with $\tilde{y} < y_c$, and that of negative ones with $y_c \leq \tilde{y}$. Then, the samples fall into the four categories in Table 1. The true-positive rate is defined as $N_{\text{TP}} / (N_{\text{TP}} + N_{\text{FN}})$, and the false-positive rate as $N_{\text{FP}} / (N_{\text{FP}} + N_{\text{TN}})$. The ROC curve is the two-dimensional plot of false-positive rate versus true-positive rate, by changing the cutoff y_c . It has better performance if the trajectory approaches the upper left corner. Therefore, the area under the ROC curve indicates the performance.

Note that, for the readability of the histograms, we use the estimated value \hat{y} after applying the transformation:

$$\tilde{y} \leftarrow 1 - |1 - \hat{y}|, \quad (17)$$

so that $\hat{y} \leq 1$.

Table 1. Confusion matrix with cutoff y_c

		True y	
		0	1
Estimated \tilde{y}	$\tilde{y} < y_c$	True-positive N_{TP}	False-positive N_{FP}
	$y_c \leq \tilde{y}$	False-negative N_{FN}	True-negative N_{TN}

4 Results and Discussion

The data sequence has dimension $d = 3$ without the lead-lag transformation, or $2d = 6$ with the lead-lag transformation. We treat profiles with depth width (the difference between the minimum and maximum depth) of more than 1000m, and each profile has approximately $N \sim 100$ observation points. The number of profiles is $M = 8.2 \times 10^4$, and each profile is converted into the signature up to order $n = 6$.

An overview of the machine learning results is shown by the histogram of estimated values \tilde{y} for accepted samples ($y = 1$), and the histogram for rejected samples ($y = 0$).

Figure 2 shows the histograms when 40% of the data records are used for training and the remaining 60% are used for cross-validation. We can see that learning is properly performed because there is little difference between the identification of learning data and the cross-validation. In particular, this approach never fails to reject negative (normal) profiles if the appropriate cutoff y_c is used, but it may accept positive (bad) profiles with a probability 0.6 when $y_c = 0.5$. This property is also reflected in the tendency of the ROC curve (Fig. 4) to be almost tangent to the $x = 0$ axis when x is small, but not tangent to $y = 1$ when y is large. The histogram for positive samples has two clear peaks, which suggests that the ambiguity is not caused by the judgment by the machine learning, but by the fact that the original quality control flag had a criterion that cannot be decided only by the shape.

Figure 3 shows the histograms when 2.5% of the data are used for training and the remainder is used for cross-validation. In this case, there is a clear tendency of over-learning, which indicates that the number of learning samples, 2.5%, is not sufficient. Comparing the results of the experiments with various ratios of learning samples by the area under the ROC curves (AUC) shows that over-learning occurs when the ratio is less than 20% (Fig. 5).

We also compared the results of the experiments with various weights α of the regularization term by the AUC. If we increase the degrees of freedom of the coefficients w by using a smaller α , the performance of the reproduction capability increases, but the estimation capability begins to saturate at approximately 6700 degrees of freedom (Fig. 6); with $\alpha = 10^{-5}$, where the complexity is at an appropriate level.

Overall, we found that machine learning using the signature method can learn the existing quality control flags of Argo profiles, and automatically assign the flag to new profiles, but it sometimes overlooks bad samples because of the ambiguity inherent in the original quality control flag.

5 Conclusions

In this research, we first showed that the shape of a profile from the Argo ocean observing array can be represented by the iterated integrals. Then, we constructed a model for the function that assigns a quality control flag to the shape of a profile, which is expressed as a weighted sum of the iterated integrals. We performed supervised learning for the weights using the existing quality control flags for training data, and demonstrated by cross-validation that it has skill in estimating flags for unknown data. This algorithm has the potential of enabling automatic assignment of quality control flags to new Argo data. The significance of the algorithm is that it objectively and automatically assigns the quality control flag only on the basis of past knowledge about the quality of data without imposing any ad hoc rules. Hence, it should enable more objective and efficient quality control compared to traditional manual methods or rule-based machine learning.

The signature method is quite effective for expressing quantitatively the shape of an Argo profile and its nonlinear function. The rationale for this conclusion is that a nonlinear and complicated function of assigning quality control flags can be transformed to a linear combination of the iterated integrals through algebraic transformation (shuffle product) without introducing any errors. This is superior to conventional multivariate regression models, which approximately regard nonlinear dependencies as linear ones. Along this line, we can express, as a function of signature, not only quality control flags, but also any oceanic phenomena.

One application of the signature method is assimilation of the signature of observational data into a general ocean circulation model. For example, we can convert a vertical sequence of observational data and that of model data into iterated integrals. We then construct a cost function that compares the signatures for model and observation, rather than directly comparing the state vectors composed of temperature and salinity at each depth. By doing so, we gain the advantage that the projection of a vertical profile onto any ocean phenomena attains a linear form, which results in efficient data assimilation. This result occurs because we can expect that many diagnoses for oceanic conditions are written in terms of iterated integrals, as illustrated in appendix A.

Appendix A: Oceanographic conditions in terms of iterated integrals

Here we show some diagnoses for oceanographic conditions that can be written in terms of iterated integrals.

1. The First-order iterated integrals are

$$X^{(1)} = \int_{u=0}^t dP_u = P_t - P_0, \quad X^{(2)} = S_t - S_0, \quad X^{(3)} = T_t - T_0,$$

which are profile length, sea surface salinity, and sea surface temperature, respectively.

2. The second-order iterated integrals include

$$X^{(11)} = \frac{1}{2}(P_t - P_0)^2, \quad X^{(12)} = \int_{u=0}^t (S_t - S_u)dP_u, \quad X^{(13)} = \int_{u=0}^t (T_t - T_u)dP_u,$$

which represent the square of profile length, total salinity content, and total heat content, respectively.

3. As an example of higher-order iterated integrals, we show here that thermal wind flow can be written with iterated integrals.

The thermal wind relation is written in vertical P -coordinates as

$$f \frac{\partial u}{\partial P} = - \frac{\partial}{\partial y} (\rho^{\bullet-1}) \Big|_{P=\text{const.}}, \quad f \frac{\partial v}{\partial P} = \frac{\partial}{\partial x} (\rho^{\bullet-1}) \Big|_{P=\text{const.}}, \quad (\text{A1})$$

where f is the Coriolis parameter, u, v are velocity, ρ is density, and x, y are the longitudinal and latitudinal coordinates, respectively. For a fixed latitude y , by performing integrations along the x direction and then the P direction, we obtain an estimate for the meridional velocity as

$$f \int_{x'=x_0}^{x_1} \frac{\partial v}{\partial P} dx' = \rho(x_1, P')^{\bullet-1} - \rho(x_0, P')^{\bullet-1} =: [\rho(x, P')^{\bullet-1}]_{x=x_0}^{x_1}, \quad (\text{A2})$$

$$f \int_{x'=x_0}^{x_1} v(x', P) dx' = \left[\int_{P'=P_0}^P \rho(x, P')^{\bullet-1} dP' \right]_{x=x_0}^{x_1}, \quad (\text{A3})$$

where we set $v(x', P_0) = 0$ as the layer of no motion. Integrating again along the P direction, we obtain the meridional flow rate as

$$\begin{aligned} Q_v &:= -g^{\bullet-1} \int_{P''=P_0}^{P_1} \int_{x'=x_0}^{x_1} v(x', P'') dx' dP'' \\ &= -(gf)^{\bullet-1} \left[\int_{P''=P_0}^{P_1} \int_{P'=P_0}^{P''} \rho(x, P')^{\bullet-1} dP' dP'' \right]_{x=x_0}^{x_1}, \end{aligned} \quad (\text{A4})$$

where the unit is in $[\text{kgs}^{\bullet-1}]$ because of the p -coordinate.

Let $\tau \in [0, 1]$ be a parameter for the order of observational points in a profile. Evaluating the density in Eq. (A4) with the state equation ϱ , we have

$$\rho(x, P)^{\bullet-1} = \varrho(T(x, \tau), S(x, \tau), P(x, \tau))^{\bullet-1} = \varrho \left(\int_0^\tau dT_{\tau'}, \int_0^\tau dS_{\tau'}, \int_0^\tau dP_{\tau'} \right)^{\bullet-1}, \quad (\text{A5})$$

which has iterated integrals as independent variables. Notice that the Shuffle-product property transcribes this as a linear combination of iterated integrals. Substituting this into Eq. (A4) finally yields

$$Q_v = -(gf)^{\bullet-1} \left[\int_{\tau_3=0}^1 \int_{\tau_2=0}^{\tau_3} \varrho \left(\int_{\tau_1=0}^{\tau_2} dT_{\tau_1}, \int_{\tau_1=0}^{\tau_2} dS_{\tau_1}, \int_{\tau_1=0}^{\tau_2} dP_{\tau_1} \right)^{\bullet-1} dP_{\tau_2} dP_{\tau_3} \right]_{x=x_0}^{x_1}. \quad (\text{A6})$$

This shows that the meridional flow rate Q_v is represented as a linear combination of iterated integrals with respect to T, S , and P .

Author contributions. SH compiled the observational data. NS proposed the method, performed the statistical analyses, and prepared the manuscript with contributions from the co-author.

Competing interests. The authors declare that they have no competing interests.

Acknowledgements. The authors appreciate the members of JAMSTEC Argo data management team for preparing and compiling the Argo profile data. All numerical computations were performed on the JAMSTEC DA supercomputer system.

References

- ARGO: Argo float data and metadata from Global Data Assembly Centre (Argo GDAC), SEANOE, <https://doi.org/10.17882/42182>, 2019.
- Chen, K.-T.: Integration of Paths—A Faithful Representation of Paths by Noncommutative Formal Power Series, *Transactions of the American Mathematical Society*, 89, 395–407, <http://www.jstor.org/stable/1993193>, 1958.
- Chevyrev, I. and Kormilitzin, A.: A Primer on the Signature Method in Machine Learning, ArXiv e-prints, 2016.
- Egan, J. P.: *Signal detection theory and ROC analysis*, Academic Press, 1975.
- Friedman, J., Hastie, T., Höfling, H., and Tibshirani, R.: Pathwise coordinate optimization, *The Annals of Applied Statistics*, 1, 302–332, 2007.
- Gould, J., Roemmich, D., Wijffels, S., Freeland, H., Ignaszewsky, M., Jianping, X., Pouliquen, S., Desaubies, Y., Send, U., Radhakrishnan, K., Takeuchi, K., Kim, K., Danchenkov, M., Sutton, P., King, B., Owens, B., and Riser, S.: Argo profiling floats bring new era of in situ ocean observations, *Eos, Transactions American Geophysical Union*, 85, 185–191, <https://doi.org/10.1029/2004EO190002>, <https://agupubs.onlinelibrary.wiley.com/doi/abs/10.1029/2004EO190002>, 2004.
- Hayashi, S., Ono, S., Hosoda, S., Numao, M., and Fukui, K.: Error Detection of Ocean Depth Series Data with Area Partitioning and Using Sliding Window, in: 2016 15th IEEE International Conference on Machine Learning and Applications (ICMLA), pp. 1029–1033, <https://doi.org/10.1109/ICMLA.2016.0186>, 2016.
- Kamikawaji, Y., Matsuyama, H., Fukui, K., Hosoda, S., and Ono, S.: Decision tree-based feature function design in conditional random field applied to error detection of ocean observation data, in: 2016 IEEE Symposium Series on Computational Intelligence (SSCI), pp. 1–8, <https://doi.org/10.1109/SSCI.2016.7849862>, 2016.
- Kormilitzin, A.: *the-signature-method-in-machine-learning*, <https://github.com/kormilitzin/>, 2017.
- Levin, D., Lyons, T., and Ni, H.: Learning from the past, predicting the statistics for the future, learning an evolving system, ArXiv e-prints, 2013.
- Lyons, T. J., Caruana, M., and Lévy, T.: *Differential Equations Driven by Rough Paths*, vol. 1908 of *Lecture Notes in Mathematics*, Springer, 2007.
- Ono, S., Matsuyama, H., Fukui, K., and Hosoda, S.: Error detection of oceanic observation data using sequential labeling, in: 2015 IEEE International Conference on Data Science and Advanced Analytics (DSAA), pp. 1–8, <https://doi.org/10.1109/DSAA.2015.7344896>, 2015.
- Pedregosa, F., Varoquaux, G., Gramfort, A., Michel, V., Thirion, B., Grisel, O., Blondel, M., Prettenhofer, P., Weiss, R., Dubourg, V., Vanderplas, J., Passos, A., Cournapeau, D., Brucher, M., Perrot, M., and Duchesnay, E.: Scikit-learn: Machine Learning in Python, *Journal of Machine Learning Research*, 12, 2825–2830, 2011.

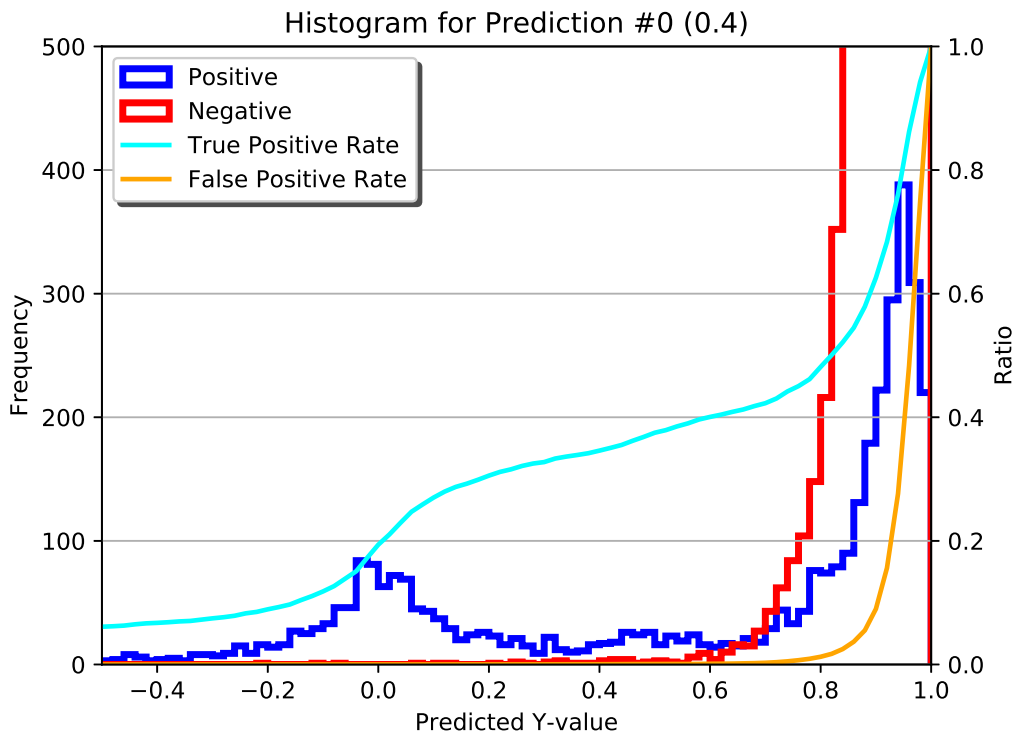
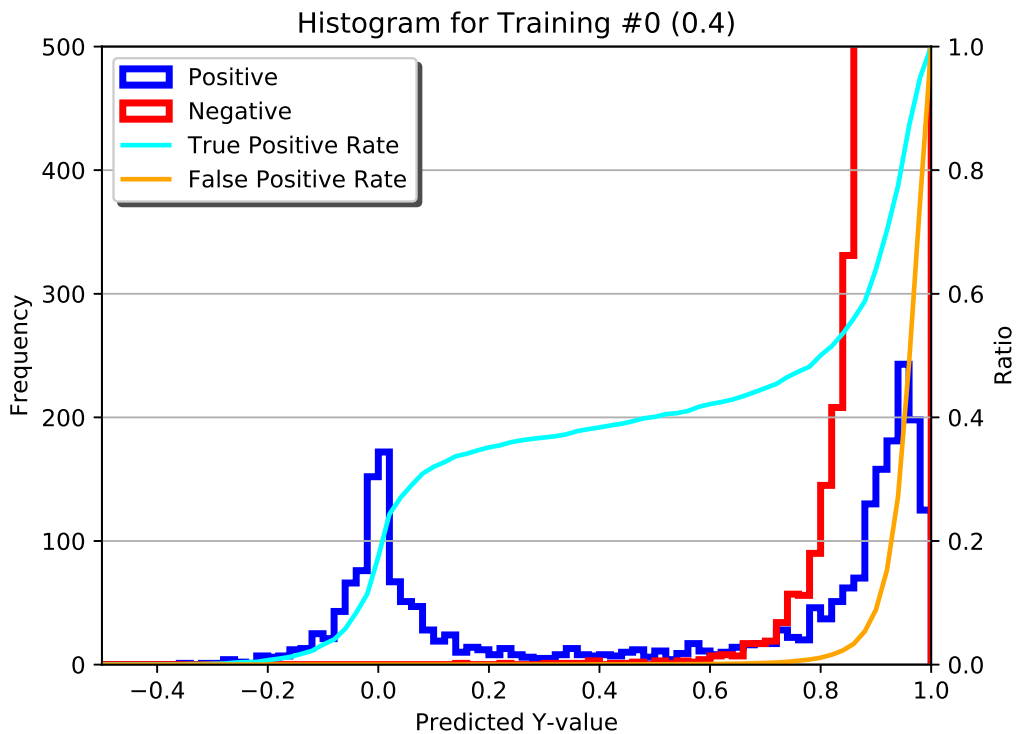


Figure 2. Histogram for discriminant analysis. Proportion of training data: 0.4, $\alpha = 10^{-5}$. Top: identification of the training data; bottom: cross-validation.

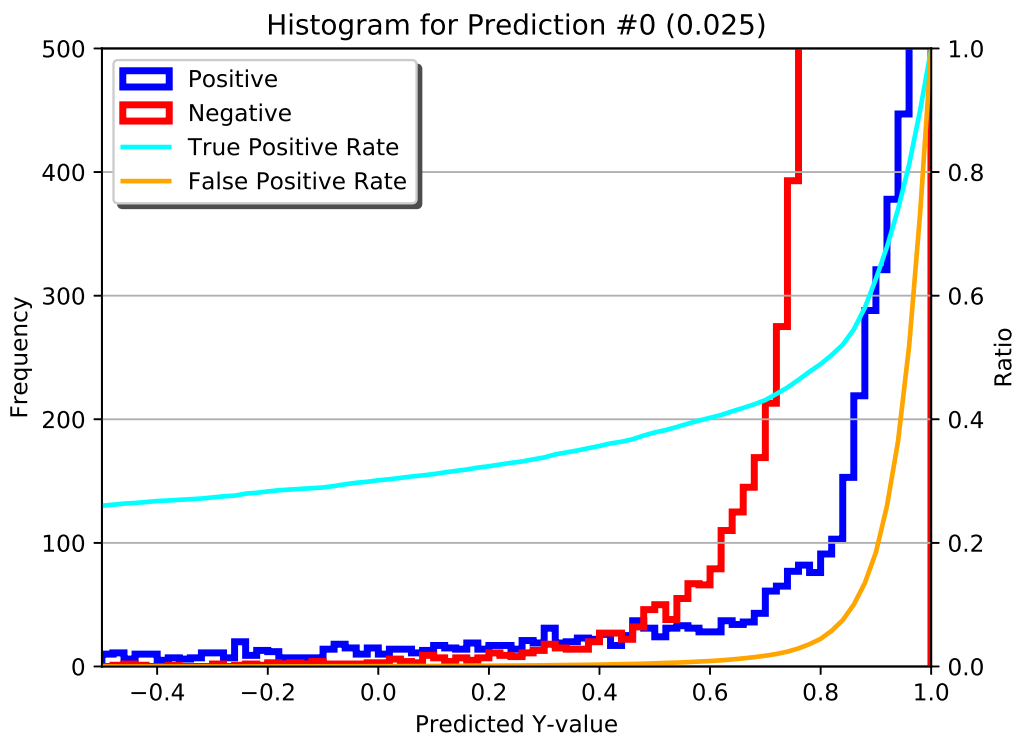
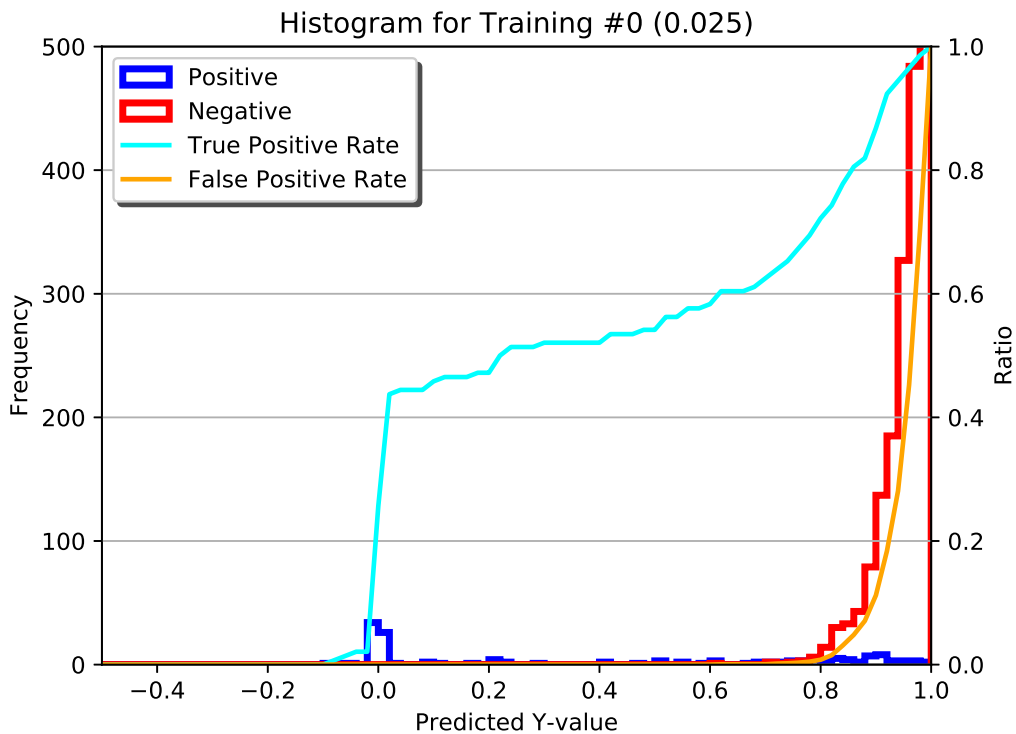


Figure 3. Histogram for discriminant analysis. Proportion of training data: 0.025, $\alpha = 10^{-5}$. Top: identification of the training data; bottom: cross-validation.

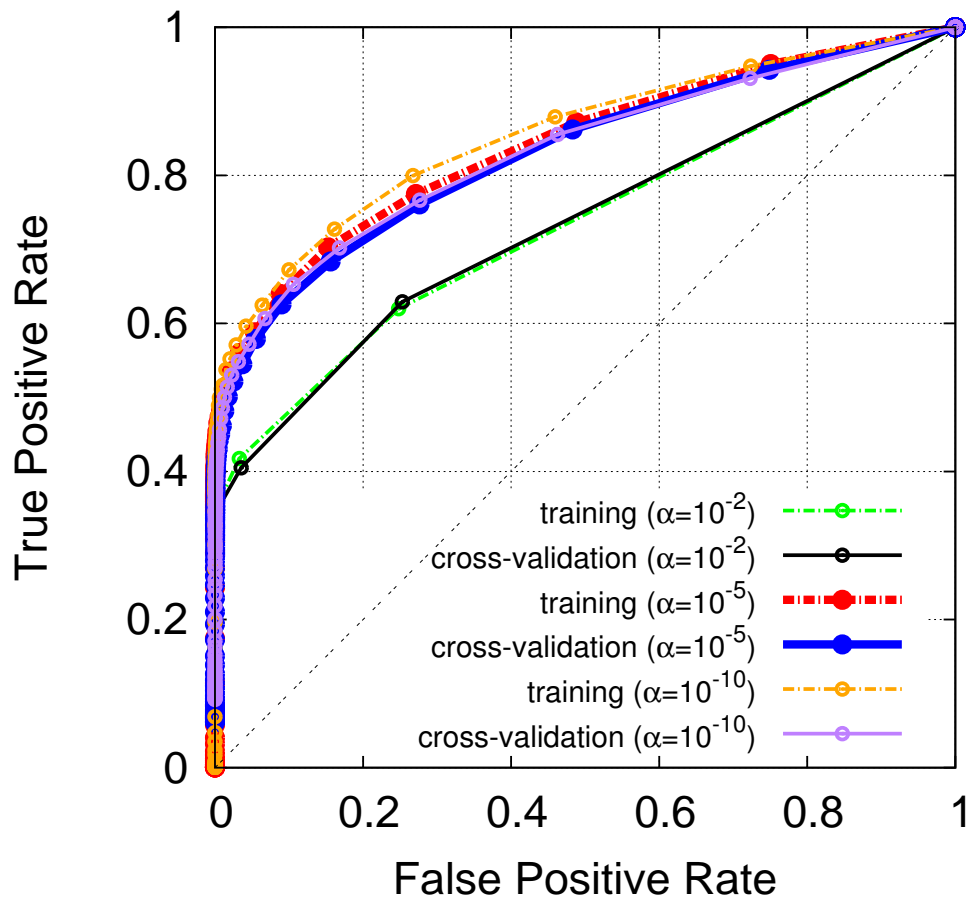


Figure 4. ROC curves for various regularization parameters.

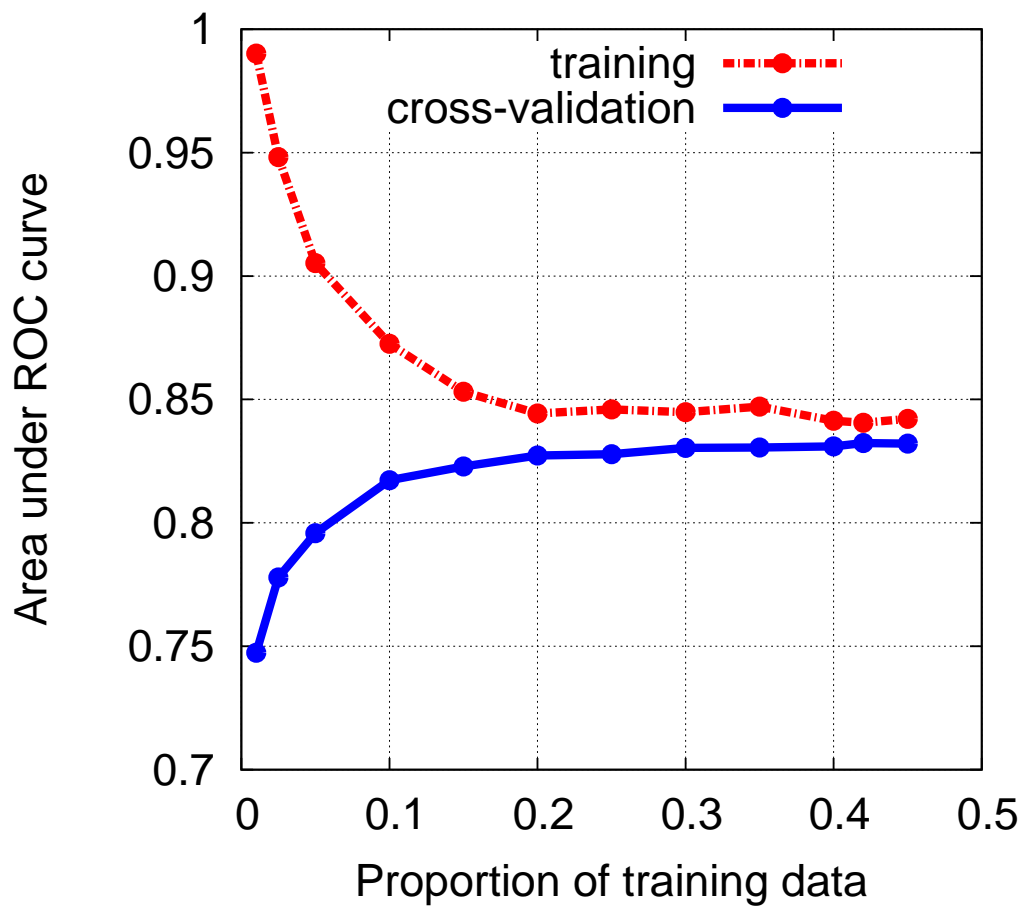


Figure 5. Learning curves for different proportions of training data. Red: identification of the training data; blue: cross-validation.

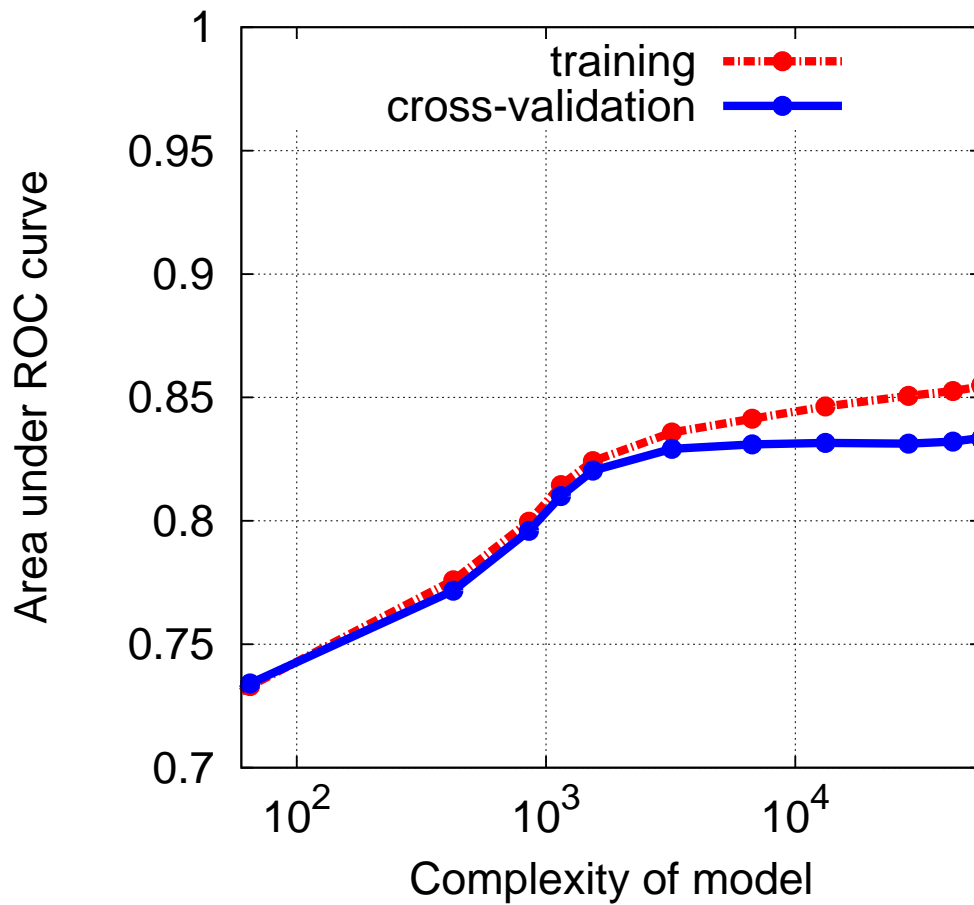


Figure 6. Learning curves for different model complexities. Red: identification of the training data; blue: cross-validation.